鐵-鈀-銀合金之磁性相微結構與磁特性
Magnetic Structure and Magnetic Property of Fe-Pd-Ag Alloys

林英志[*1] 李驊登[1] 林建鋒[2]
Yin-Chih Lin[*1], Hwa-Teng Lee[1], Chien-Feng Lin[2]

摘要

本研究論文主要利用穿透式電子顯微鏡(TEM)，X-ray繞射儀，調幅式示差掃描量熱計(DSC)，與超導量子干涉磁化儀(SQUID)，探討鐵-30鈀-4銀磁性合金固溶處理，與固溶處理後再經400-500℃，時效於各種不同時間之磁性相微結構與磁特性關係，TEM、X-ray繞射與DSC實驗結果證實，此合金固溶與時效處理後，在fcc → $L1_0$麻田散鐵相變態間，存在一中間相，此中間相為$L1_m$單斜晶結構，其晶格常數為 $a = 3.208$ Å, $b = 3.696$ Å, $c = 3.127$ Å, 及 $\beta = 91.997°$，此中間相可能為一種適性相麻田散鐵。

超導量子干涉磁化儀之磁性量測結果顯示，固溶處理試樣，其ZFC與FC之磁化曲線並不聚合，一直到室溫$T_R = 300$K，當試樣固溶處理，再經500℃/100小時之時效處理後，則其ZFC與FC之磁化曲線呈現鋸齒狀(serrated)，此現象表示有兩種磁性相，存在時效處理之試樣內部，此兩種磁性相包括單斜晶$L1_m$與序化型正方晶$L1_0$微結構，這兩種磁性相具有不同之磁異向性(magnetic anisotropy)。

關鍵詞：鐵-鈀-銀合金，TEM與X-ray繞射，DSC，中間相$L1_m$微結構

Abstract

This investigation reports on TEM, X-ray diffraction, DSC, and SQUID magnetometer study of magnetic structures formed in Fe-30Pd-4Ag alloys solution treated and then thermally aged at 400-500℃ for various times. The results reveal that an intermediate structure appears between the fcc → $L1_0$ martensitic transformation. The intermediate phase, denoted $L1_m$, has a monoclinic structure with lattice parameters of $a = 3.208$ Å, $b = 3.696$ Å, $c = 3.127$ Å, and $\beta = 91.997°$, which indicates that the monoclinic structure is possibly adaptive martensite, as confirmed by TEM, X-ray diffraction, and DSC.

The SQUID test shows that the ZFC and FC curves of the ST specimen do not coalesce until they reach room temperature at $T_R = 300$ K. The serrated ZFC and FC curves of the specimen aged at 500℃ for 100 h indicate that two phases exist in the aged specimen. The two phases are comprised of monoclinic $L1_m$ phase and tetragonal ordered $L1_0$ structure, which have differing magnetic anisotropy.

Keywords: Fe-Pd-Ag alloys, TEM and X-ray diffraction, DSC, Intermediate $L1_m$ structure

I. INTRODUCTION

Ferromagnetic shape memory alloys (FSMAs) have recently attracted attention for application as a magnetic actuator material. In FSMAs, a large strain by magnetic field-induced twinning/detwinning has been discovered [1-2]; in addition, FSMAs can achieve a large displacement and quick response by magnetic field-induced $L1_0$ martensitic transformation or by magnetic field-induced rearrangements of $L1_0$ martensitic twinning magnetostriction. Therefore, FSMAs will become the most potential actuator material for magneto-mechanical applications in the near future [1-2]. At the moment, several systems of FSMAs, such as Ni-Mn-Ga, Co-Ni-Al, Fe-Pt, and Fe-Pd, have been attracting much more research. Among these alloy systems, the Fe-Pd alloys have a better mechanical property (ductility), a higher Curie temperature (~500℃),

[1] 國立成功大學機械工程研究所 [2] 崑山科技大學機械工程研究所
[*]Corresponding author. E-mail: lin3312@cc.kuas.edu.tw
[1] Department of Mechanical Engineering, National Cheng Kung University, Tainan, Taiwan, R.O.C.
[2] Department of Mechanical Engineering, Kun Shan University of Technology, Tainan, Taiwan, R.O.C.
Manuscript received 9 November 2007; accepted 25 January 2008

and a large magnetization anisotropy constant (K_1= 1.45×10^7 ergs/cm^3). Despite the disadvantage of this alloy, namely the limited stability of the $L1_0$ phase, it is possible both to extend the stability range of the $L1_0$ martensite and to improve the softness of the Fe-Pd alloys with the addition of a third alloy element. Addition of the third element can usually induce a strong influence on the $L1_0$ martensitic transformation [3]. Therefore, in this study, we select Ag as the third alloy element for the Fe-Pd alloys. The $L1_0$ martensitic transformation and magnetic property of the composition Fe-30Pd-4Ag alloys are investigated in the present work.

II. EXPERIMENTAL PROCEDURE

The Fe-30Pd-4Ag (at%) alloys were formed by melting by pure electrolytic iron (99.9%), pure palladium (99.95%), and pure silver (99.95%) in an arc vacuum furnace under a controlled protective argon atmosphere. The cast ingots were sealed in evacuated quartz capsules and homogenized at 1050°C for 60 hours and subsequently forged to a thickness of 2~3mm. After forging, the specimens were sliced and sealed in evacuated quartz capsules again and solution treated (ST) at 950°C for 1.5 hours before being quenched in ice water. The aging treatment was performed in the temperatures range of 400-550°C for various amounts of time. Thin foils for TEM were prepared by double jet electropolishing in a solution containing 82% acetic acid, 9% perchloric acid, and 9% methanol at a temperature in the range of -7°C~10°C using a current density of 2A/cm^2 to 4A/cm^2. Transmission electron microscopy (TEM), with a double tilt stage, was performed in an analytical type high resolution electron microscope (Hitachi HF-2000) with a field emission gun operated at 200 kV, and a JEM-2100F operated at 200 kV, respectively. The X-ray diffraction patterns were detected at room temperature using an X-ray diffractometer (Siemens D5000 Karlsruhe) with Cu-Kα radiation, and diffraction angles were in the 2θ ranges from 35° to 140°. The martensitic phase transformation temperatures of the samples that were only solution treated and those that were solution treated and then thermally aged were determined with differential scanning calorimetry (2920 MDSC V2.6A). A temperature range from -50 to 220℃ was scanned at a rate of 10℃/min during heating. (i.e., The samples were scanned in a temperature range from -50 to 220℃ at a heating rate of 10℃/min). The magnetic property zero-field-cooled (ZFC) and field-cooled (FC) measurements were carried out with a superconducting quantum interference device (SQUID) magnetometer. The temperature dependence of mass susceptibility (χ where χ = M/ρH, ρ = density) measurements on samples cooled under 20000 Oe were made in the temperature range from 0 K to 350 K by induction method.

III. RESULTS AND DISCUSSION

1. γ_{fcc} phase transformation into the monoclinic $L1_m$ phase+$L1_0$ structure observed by TEM

Figure 1(a) shows an essential transmission electron microscopy (TEM) selected area diffraction pattern (SADP) with zone axis $[011]_{L10}//[\bar{2}\,\bar{3}\,2]_{L1m}$ of the Fe-30Pd-4Ag alloy solution treated (ST) at 950°C for 1.5 h and quenched in ice water (*hkl* denotes the ordered $L1_0$ phase; $\underline{hkl}$ denotes the monoclinic $L1_m$ structure). On the basis of the diffraction pattern analysis, a dim satellite spot beside the $\{200\}_{L10}$ position can be seen in the SADP micrograph, an indication that the as-quenched γ_{fcc} phase separation into the $L1_0$ structure should be a weak first ordering reaction [4-5]. This first ordering reaction begins during the solution treatment (ST) and quenching in ice water. Figure 1(b) is a dark field (DF) image formed using the $(1\,\bar{1}\,1)_{L10}$ reflection corresponding to Fig. 1(a). In this image, the first ordered $L1_0$ structure, in bright contrast with a twinned structure (tetragonal), can be distinctly observed in the early phase transition. Figure 1(c) is a dark field (DF) image formed using the $(\underline{2\,\bar{2}\,1})_{L1m}$ monoclinic reflection corresponding to Fig. 1(a). The DF image of Fig. 1(c) reveals that the initial intermediate $L1_m$ monoclinic phases

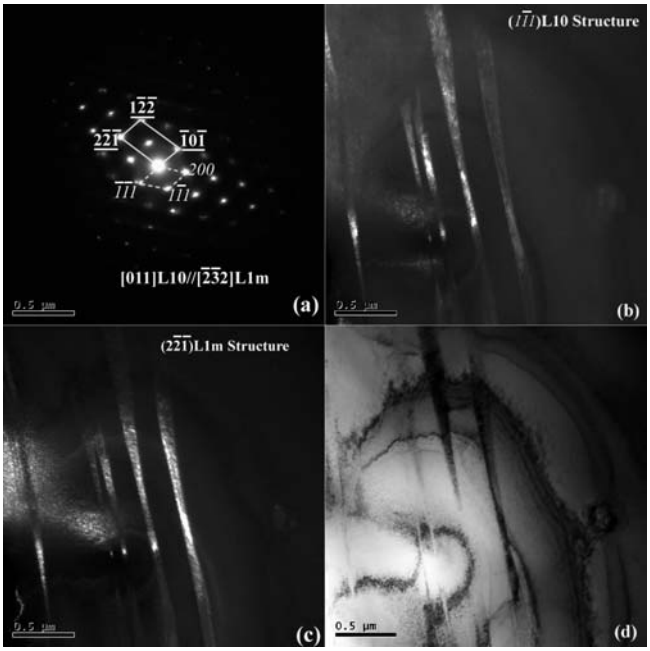

Fig. 1 TEM micrographs of the Fe-30Pd-4Ag alloys solution treated (ST) at 950 ℃ for 1.5 h and quenched in ice water: (a) SADP of the zone axis $[011]_{L10}//[\bar{2}\,\bar{3}\,2]_{L1m}$ (*hkl* denotes the ordered $L1_0$ phase; $\underline{hkl}$ denotes the monoclinic $L1_m$ structure), (b) DF image of $(1\,\bar{1}\,1)_{L10}$ ordered $L1_0$ reflection corresponding to (a), (c) DF image for $(\underline{2\,\bar{2}\,1})L1_m$ reflection corresponding to (a), (d) BF image

are comprised of modulated structures with tiny antiphase boundaries (APBs). Figure 1(d) is a bright field (BF) struture. The SADP of the TEM micrograph taken from the alloy ST then thermally aged at 450°C for 100 h is shown in Fig. 2(a), in which the zone axis reveals the $[\bar{1}12]_{L10}//[4\ \bar{1}\ 3]_{L1m}$ (*hkl* denotes the ordered $L1_0$ phase; hkl denotes the monoclinic $L1_m$ structure). The two phases' reflection spots are clearly shown in the SADP image (Fig. 2(a)). By calculating the X-ray diffraction d-spacing in association with the SADP image measurements, it is found that the adaptive $L1_m$ martensite has a monoclinic structure with lattice parameters of a = 3.208 Å, b = 3.696 Å, c = 3.127 Å, and β = 91.997°, and the ordered $L1_0$, a normal martensitic structure with lattice parameters of a = 3.878 Å, c = 3.696 Å, and c/a= 0.953.

Figure 2(b) is a dark field (DF) image formed using the monoclinic $(\bar{1}\ \bar{1}\ 1)_{L1m}$ reflection corresponding to Fig. 2(a). The DF image in Fig. 2(b) reveals that the intermediate $L1_m$ monoclinic phases are comprised of microtwins and antiphase boundaries (APBs). These planar faults strongly support the mechanism of coercivity in the aged Fe-Pd-Ag alloy system; it has tended to favor microtwins and APBs pinning the magnetic domain wall motion, which has been illustrated as a possible source of magnetic hardening [6-8]. Figure 2(c) is a bright field (BF) image. For further confirmation of the existence of two phases in the aged alloy, a high resolution TEM (HRTEM) image (Fig. 2(d)) taken from the same specimen shows the presence of the monoclinic $L1_m$ structure with an ordered $L1_0$ phase, and the antiphase boundaries (APBs – i.e., the faint black curved image) in the matrix, as indicated by an arrow. Due to the appearance of the APBs, the aged $L1_0$ phase should be reasonably inferred as a second ordered structure, and the APBs pinning the magnetic domain wall motion are further demonstrated as a possible source of magnetic hardening of the alloy after ST followed by thermal aging. By careful measurements of the lattice space of Fig. 2(d), it is found that the d-spacing of the monoclinic $L1_m$ structure is 2.38 Å, and the ordered $L1_0$ phase is 2.2 Å; therefore, the plane (Fig. 2(d)) can be reasonably inferred to be $(011)_{L1m}$ and $(111)_{L10}$, respectively.

2. X-ray diffraction pattern analysis

Figures 3(a)-(c) represent a series of X-ray diffraction patterns of the alloys that were solution treated and those solution treated and then thermally aged at 400°C and 475°C for various times. The X-ray diffraction pattern of the alloy ST at 950°C for 1.5 h and quenched in ice water

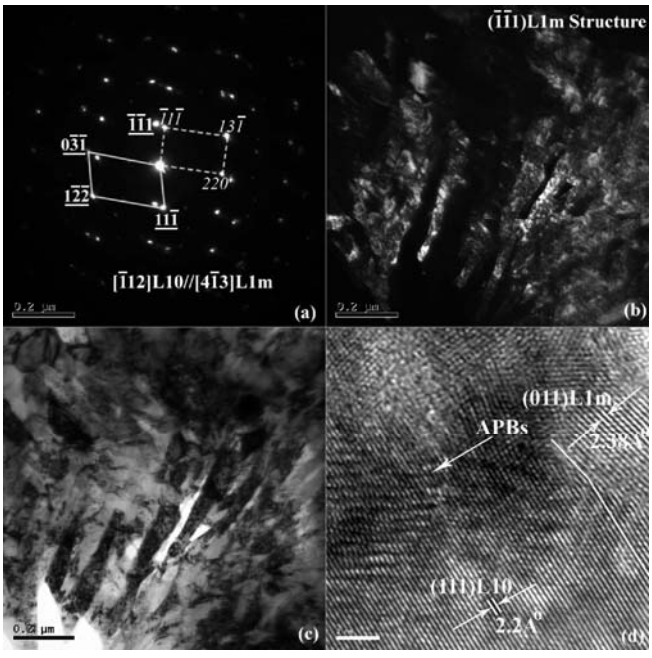

Fig. 2 TEM micrographs of the Fe-30Pd-4Ag alloys ST and aged at 450 ℃ for 100 h: (a) SADP of the zone axis $[\bar{1}12]_{L10}//[4\ \bar{1}\ 3]_{L1m}$ (*hkl* denotes the ordered $L1_0$ phase; hkl denotes the monoclinic $L1_m$ structure), (b) DF image for $(\bar{1}\ \bar{1}\ 1)L1_m$ reflection corresponding to (a), (c) BF image, (d) high resolution TEM (HRTEM) micrograph showing the antiphase boundaries (APBs) and two phases' d-spacing

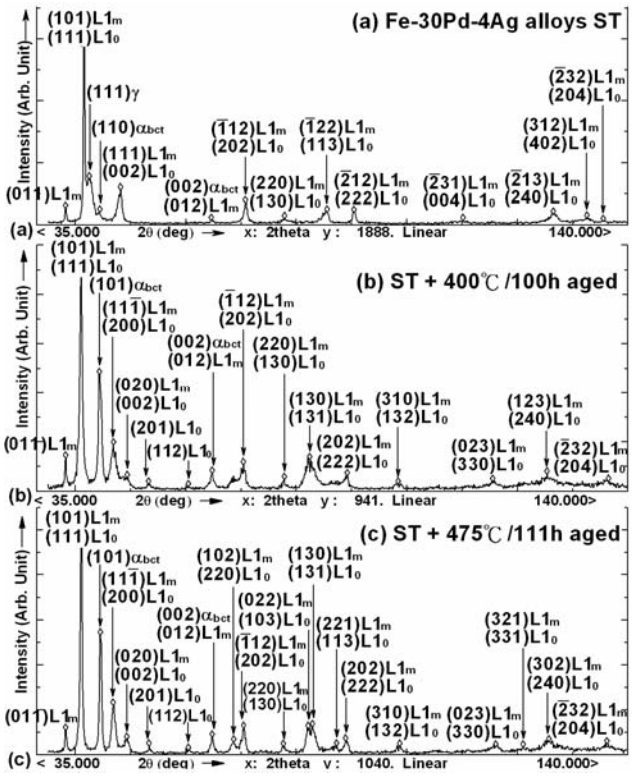

Fig. 3 X-ray diffraction patterns of the alloy solution treated and those ST and then thermally aged at 400 and 475 °C for given times: (a) 950 °C for 1.5 h ST and quenched in ice water, (b) ST and aged at 400 °C for 100 h, and (c) ST and aged at 475 °C for 111 h. (α_{bct} denotes the body centered tetragonal martensite, $L1_m$ denotes the adaptive $L1_m$ monoclinic structure, and $L1_0$ denotes the ordered $L1_0$ martensitic phase)

is shown in Fig. 3(a), in which reflections of two phases $(101)_{L1m}$ and $(111)_{L10}$ are the main diffraction peak. The $(111)_{\gamma}$ and $(110)_{\alpha bct}$ peaks also appear; in addition, there is an observable $(011)_{L1m}$ peak in the X-ray diffraction pattern. The X-ray experiment results exhibit that an intermediate structure appears between the fcc → $L1_0$ martensitic transformation, which occurs in the early ST treatment. Simultaneously, the X-ray experiment also demonstrates that the addition of silver (Ag) to the Fe-Pd alloy system enhances the $L1_m$ and $L1_0$ phase formation. When the alloy is aged at 400°C for 100 h, many adaptive $L1_m$ monoclinic structures and ordered $L1_0$ martensitic phases appear in the X-ray diffraction patterns, in addition to the $(111)_{\gamma}$ phase separation to the $(110)_{\alpha bct}$+$L1_m$+$L1_0$ structures, as shown in Fig. 3(b). It is also interesting to note that the X-ray diffraction peak for the plane $(002)_{L10}$, $(202)_{L10}$, $(113)_{L10}$ reflections corresponding to the ST specimen in Fig. 3(a) have been transformed into the tetragonal splitting peak $(200)_{L10}$;$(002)_{L10}$, $(220)_{L10}$;$(202)_{L10}$, and $(131)_{L10}$;$(113)_{L10}$ reflections when the specimen has been aged at 475°C for 111 h, as shown in Fig. 3(c). These splitting peaks are the result of the formation of the completely ordered tetragonal $L1_0$ martensitic structures attendant on the $L1_m$ → $L1_0$ phase transformation reaction. Comparison of the $L1_0$ tetragonal splitting peaks of Figs. 3(b) and 3(c) reveals that the axial ratio c/a of the ordered $L1_0$ martensite gradually decreased when the aging temperature was lowered to 400°C. On the other hand, the degree of tetragonality develops as the specimen is aged at a lower temperature of 400°C, in which case it gives rise to an increase in the anisotropy and enhances the magnetic coercivity in the Fe-Pd-Ag alloy [9-11].

3. Martensite $L1_0$ phase transformation temperature

Martensitic $L1_0$ phase transformation temperatures of the specimen ST at 950℃ for 1.5 h and quenched in ice water were determined by differential scanning calorimetry (DSC). The results are shown in Fig. 4(a). Two distinct peaks in the heating direction are observed, indicating a two-step phase transition [12-13]. The first endothermic peak in the heating direction corresponds to the superposition of the $L1_m$ (monoclinic phase)+A (austenite structure) with $L1_{ms}$ = 24.86℃, $L1_{mf}$ = 52℃, A_s = 28℃, and A_f = 54℃. The subscript "s" denotes the temperature at which the phase transformation starts, and the "f" denotes the temperature at which the phase transition finishes. The second DSC peak (i.e., the exothermic peak) corresponding to the second ordered $L1_0$ martensite phase is determined to have transformation temperatures M_{L10s} = 183℃ and M_{L10f} = 204℃ (here M_{L10s} denotes the second ordered $L1_0$ martensite phase transition start). The DSC study indicates the martensitic phase transition during heating as follows; a weak first ordered $L1_0$ martensite → $L1_m$ (monoclinic phase) → A (austenite structure) → second ordered $L1_0$ martensite. From the DSC chart, it is inferred that the $L1_m$ phase transforms to second ordered $L1_0$ martensite in addition to the direct transformation from A (austenite) to second ordered $L1_0$ martensite during heating of the sample. Figure 4(b) shows a DSC heating curve of a specimen ST and then thermally aged at 475℃ for 111 h. The DSC chart reveals two endothermic peaks and one exothermic peak during heating. This is referred to as a three-step transformation on heating [14-15]. Two endothermic peaks correspond to the $L1_m$ (monoclinic phase) and A (austenite structure) with $L1_{ms}$ = 12.5℃, $L1_{mf}$ = 18℃, A_s = 19.4℃, and A_f = 37.5℃, respectively. The one exothermic peak indicating the second ordered $L1_0$ martensite phase was determined to have transformation temperatures M_{L10s} = 156℃ and M_{L10f} = 162.5℃. Comparison of the DSC chart of Fig. 4(a) with Fig. 4(b) indicates that when the specimen was ST and then thermally aged at 475℃ for 111 h (Fig. 4(b)), the phase transition temperatures of the $L1_m$ (monoclinic structure), the A (austenite phase), and the second ordered $L1_0$ martensite phase transformation moved toward the lower temperature, concurrent with the transition heat flow peak intensity also decreasing. An intermediate structure appearing between the fcc → $L1_0$ martensitic transformation, confirmed by TEM

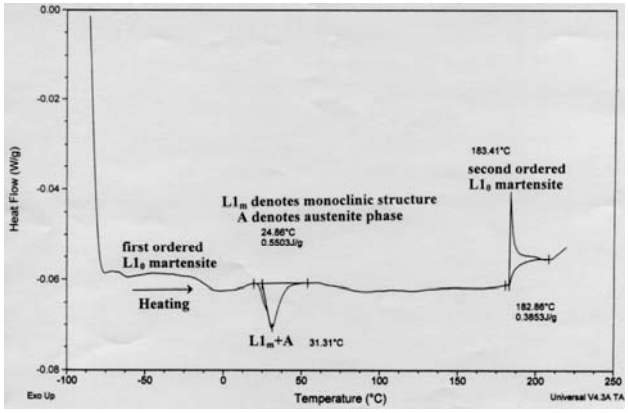

(a)

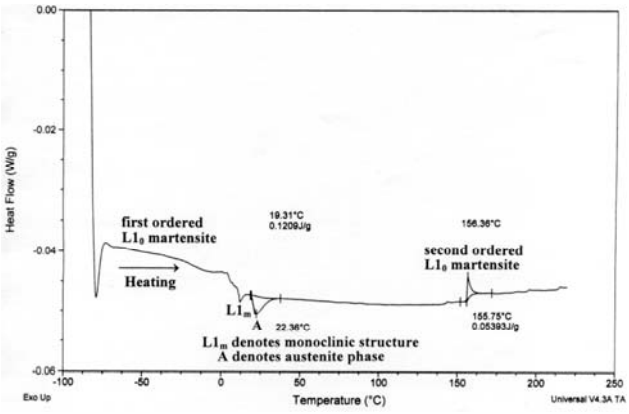

(b)

Fig. 4 DSC curves of Fe-30Pd-4Ag alloys (a) ST, (b) ST then thermally aged at 475 ℃ for 111 h, indicating that a three-step phase transformation occurred during heating the aged sample

and X-ray diffraction, is discussed in the above Section. The results of TEM and X-ray diffraction with DSC analysis are exactly coincident [16].

4. Magnetic property

Figure 5 shows the temperature dependence of the magnetic mass susceptibility (χ = M/ρH, where ρ = density) of the alloy ST at 950℃ for 1.5 h and quenched in ice water, as measured by SQUID. The measured values display both the zero-field-cooled (ZFC) data and the field-cooled (FC) data within a field of 20000 Oe. Figure 5 indicates the tendency of the ZFC and FC data for χ-T curves to decrease as the temperature increases. The ZFC data for the χ-T curve progressively decreases as 1/T, in accordance with the Curie-Weiss law [17]. In Fig. 5, it is also found that the tiny peak in the mass susceptibility-temperature (χ-T) curve occurs when the blocking temperature (T_B) is near 70 K (T_B = 70 K) for the ZFC data. It is interesting to note that in Fig. 5, the ZFC and FC curves do not coalesce above the blocking temperature (T_B = 70 K) until they reach room temperature at T_R = 300 K. Furthermore, the ZFC data lies above the FC data all the way to room temperature. This result is explained as follows: Upon cooling of the sample in a magnetic field (20000 Oe), the magnetic particles become un-trapped (i.e., unblocked) in their higher-magnetized state and have the thermal energy required to pass over the potential barriers to return to their lower-magnetized equilibrium configuration [18]. The ZFC and FC curves measured by SQUID for the alloy ST and then thermally aged at 500℃ for 100 h are shown in Fig. 6. This χ-T curve for the ZFC and FC data measurements were also performed in a magnetic field of 20000 Oe. Figure 6 gives an indication that the blocking temperature (T_B) for the aged sample is not clear. The serrated (edge and step) ZFC and FC curves occur in the specimen aged at 500℃ for 100 h, which indicates that two phases exist in the aged sample. The two phases are comprised of monoclinic $L1_m$ phases and tetragonal ordered $L1_0$ structures, which have differing magnetic anisotropy.

IV. CONCLUSIONS

1. TEM selected area diffraction pattern (SADP) reveals that the orientation relationships between the $L1_0$; $L1_m$ can be demonstrated as $[011]_{L10}//[\bar{2}\,\bar{3}\;2]_{L1m}$ and $[\bar{1}12]_{L10}//[4\;\bar{1}\;3]_{L1m}$, respectively.

2. The DSC study indicates the martensitic phase transition during heating of the sample as follows; a weak first ordered $L1_0$ martensite → $L1_m$ (monoclinic phase) → A (austenite structure) → second ordered $L1_0$ martensite.

3. The serrated (edge and step) ZFC and FC curves revealed in the aged specimen illustrate that two phases exist in the aged sample. The two phases are comprised of monoclinic $L1_m$ phases and tetragonal ordered $L1_0$ structures, which have differing magnetic anisotropy.

ACKNOWLEDGEMENTS

The authors would like to express their sincere appreciation to the National Science Council of the R.O.C. for supporting this work (under Grant-in-Aid for project No. NSC-95-2221-E-151-063).

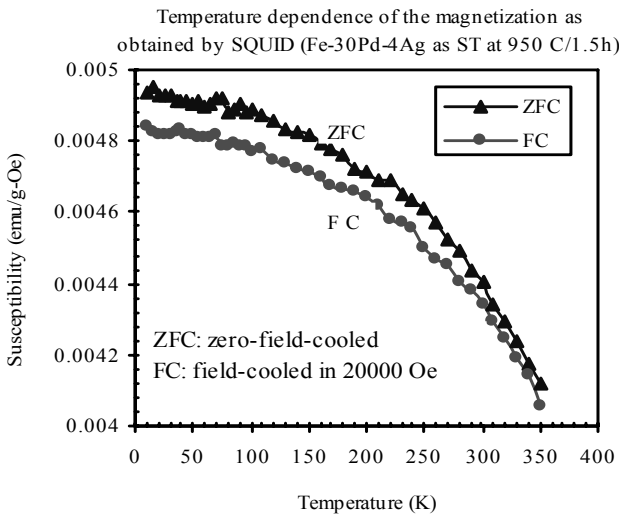

Fig. 5 Temperature dependence of the magnetic susceptibility of the alloys solution treated (ST) at 950 ℃ for 1.5 h and quenched in ice water. The measurements were carried out both at zero-field-cooling (ZFC), and at field-cooling (FC) in a field of 20000 Oe

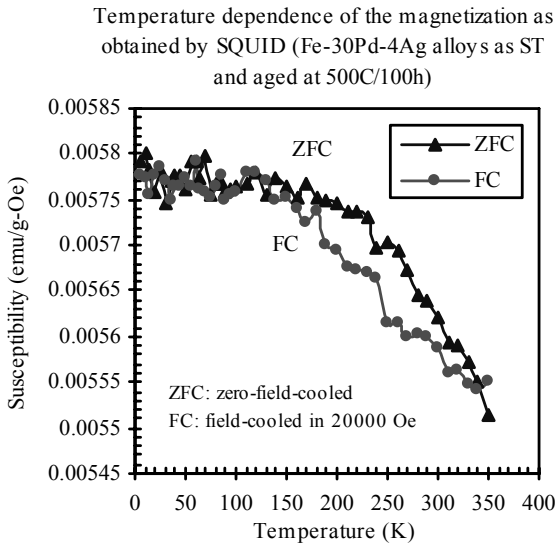

Fig. 6 Temperature dependence of the magnetic susceptibility of the alloys ST and thermally aged at 500 ℃ for 100 h. The measurements were carried out both at zero-field-cooling (ZFC), and at field-cooling (FC) in a field of 20000 Oe

REFERENCES

[1] T. Wada, T. Tagawa and M. Taya, "Martensitic transformation in Pd-rich Fe-Pd-Pt alloy," *Scripta Materialia*, vol. 48, pp. 207-211, 2003.

[2] H. Kato, Y. Liang and M. Taya, "Stress-induced FCC/FCT phase transformation in Fe-Pd alloy," *Scripta Materialia*, vol. 46, pp. 471-475, 2002.

[3] K. Tsuchiya, T. Nojiri, H. Ohtsuka and M. Umemoto, "Effect of Co and Ni on martensitic transformation and magnetic properties in Fe-Pd ferromagnetic shape memory alloys," *The Japan Institute of Metals*, Materials Transactions, vol. 44, pp. 2499-2502, 2003.

[4] J. J. Felten, T. J. Kinkus, A. C. E. Reid, J. B. Cohen and G. B. Olson, "Solid-solution structure and the weakly first-order displacive transformation in Fe-Pd alloys," *Metallurgical and Materials Transactions A*, vol. 28A, pp. 527-536, 1997.

[5] H. Xu and J. M. K. Wiezorek, "Transmission electron microscopy of room temperature deformed polytwinned $L1_0$-Ordered FePd," *Acta Materialia*, vol. 52, pp. 395-403, 2004.

[6] T. J. Klemmer, D. Hoydick, H. Okumura, B. Zhang and W. A. Soffa, "Magnetic hardening and coercivity mechanisms in $L1_0$ ordered FePd ferromagnets," *Scripta Metallurgica et Materialia*, vol. 33, pp. 1793-1805, 1995.

[7] T. J. Klemmer, C. Liu, N. Shukla, X. W. Wu, D. Weller, M. Tanase, D. E. Laughlin and W. A. Soffa, "Combined reactions associated with $L1_0$ ordering," *Journal of Magnetism and Magnetic Materials*, vol. 266, pp. 79-87, 2003.

[8] T. Sohmura, R. Oshima and F. E. Fujita, "Thermoelastic FCC-FCT martensitic transformation in Fe-Pd alloy," *Scripta Metallurgica*, vol. 14, pp. 855-856, 1980.

[9] T. Okazaki, H. Nakajima and Y. Furuya, "Large magnetostriction of Fe-29.6 at% Pd alloy ribbon under tensile stress," *The Japan Institute of Metals, Materials Transactions*, vol. 44, no. 44. pp. 665-668, 2003.

[10] T. Sakamoto, T. Fukuda, T. Kakeshita, etal, "Influence of magnetic field direction on rearrangement of martensite variants in an Fe-Pd alloy," *The Japan Institute of Metals, Materials Transactions*, vol. 12, pp. 2495-2498, 2003.

[11] E. C. Oliver, T. Mori, M. R. Daymond and P. J. Withers, "Neutron diffraction study of stress-induced martensitic transformation and variant change in Fe-Pd," *Acta Materialia*, vol. 51, pp. 6453-6464, 2003.

[12] L. Tan and W. C. Crone, "In situ TEM observation of two-step martensitic transformation in aged NiTi shape memory alloy," *Scripta Mater*, vol. 50, pp. 819-823, 2004.

[13] V. A. Chernenko, J. Pons, E. Cesari and I. K. Zasimchuk, "Transformation behavior and martensite stabilization in the ferromagnetic Co-Ni-Ga heusler alloy," *Scripta Mater*, vol. 50, pp. 225-229, 2004.

[14] C. Segui, V. A. Chernenko, J. Pons, E. Cesari, V. Khovailo and T. Takagi, "Low temperature-induced intermartensitic phase transformations in Ni-Mn-Ga single crystal," *Acta Materialia*, vol. 53, pp. 111-120, 2005.

[15] C. Jiang, Y. Muhammad, L. Deng, W. Wu and H. Xu, "Composition dependence on the martensitic structures of the Mn-rich Ni-Mn-Ga alloys," *Acta Materialia*, vol. 52, pp. 2779-2785, 2004.

[16] Y. C. Lin, H. T. Lee, S. U. Jen and Y. T. Chen, "Magnetic structure of an Fe-Pd-Rh alloy," *Journal of Applied Physics*, vol. 101, no. 9, 09N514, 2007.

[17] B. D. Cullity, *Introduction to Magnetic Materials*, ed. by M. Cohen, Addison-Wesley, Reading, Massachusetts, USA, chap.1-2, 1972.

[18] B. J. Hickey, M. A. Howson, S. O. Musa, G. J. Tomka, B. D. Rainford and N. J. Wiser, "Superparamagnetism in melt-spun CuCo granular samples," *Magn. Magn. Mater*, vol. 147, pp. 253-259, 1995.